Functional specialization and structured representations for space and time in prefrontal cortex

Claudia Böhm[1] and Albert K. Lee[1]

[1]Howard Hughes Medical Institute, Janelia Research Campus, Ashburn, United States

Correspondence: boehmc@janelia.hhmi.org, leea@janelia.hhmi.org

ABSTRACT

Individual neurons in prefrontal cortex – a key brain area involved in cognitive functions – are selective for variables such as space or time, as well as more cognitive aspects of tasks, such as learned categories. Many neurons exhibit mixed selectivity, that is, they show selectivity for multiple variables. A fundamental question is whether neurons are functionally specialized for particular variables and how selectivity for different variables intersects across the population. Here, we analyzed neural correlates of space and time in rats performing a navigational task with two behaviorally important categories – starts and goals. Using simultaneous recordings of many medial prefrontal cortex (mPFC) neurons during behavior, we found that population codes for elapsed time were invariant to different locations within categories, and subsets of neurons had functional preferences for time or space across categories. Thus, mPFC exhibits structured selectivity, which may facilitate complex behaviors by efficiently generating informative representations of multiple variables.

INTRODUCTION

Any event we experience occurs at a particular time and place. To learn about the world, make predictions, and prepare the appropriate actions to execute at the appropriate times and places, we need mechanisms to keep track of time, know where we are, and be aware of the currently relevant context. The prefrontal cortex (PFC) has been shown to encode both space[1,2] and time, for instance in temporal discrimination and reproduction tasks[3–5] or during delays[6,7]. As a key brain area involved in cognitive functions, prefrontal cortex also represents information that requires abstraction from sensory information, such as behaviorally relevant categories and rules of the task to be performed in the present context[8–10]. Thus, depending on task demands, at any moment in time during behavior in a task PFC neurons hold information about the values of a combination of variables. How does prefrontal cortex represent these key types of information and what are the neural correlates of combined variables? An understanding of the organizational principles of neural selectivity in PFC could help us understand how this information is used to enable space-, time-, and context-dependent behavior.

Individual neurons in PFC have in general been found to encode not a single variable, such as a particular stimulus or feature, but instead are often selective for multiple variables ("mixed selectivity")[11] and modulate their firing preference to changing circumstances, contexts, or rules[12]. On the other hand, recent experimental work has shown that neurons in many areas are specialized for processing specific kinds of information[13–15], and theoretical work has explored the benefits and conditions under which functional specialization might arise[16,17]. However, so far, in the medial prefrontal cortex (mPFC), evidence for functional specialization, including biases in mixed selectivity, is scant. In particular, we lack an understanding of how the selectivity of individual neurons or populations of neurons intersects with higher-order

representations (e.g. categories), a hallmark of prefrontal cortex. For instance, while PFC activity has been shown to encode space in the form of a neural correlate of the animal's current location, and categories (e.g. types of locations) as well as time, it is not clear whether the representation of time is unique at every location or transferrable to different locations or across categories. Fundamentally, the question is whether individual neurons, despite their tendency to encode multiple variables, still display biases (i.e. are specialized) to encode a particular type of information, and how the representation of one variable is impacted when another variable takes on different values.

To investigate how cognitive variables (here, categories of spatial locations) intersect with environmentally (place) or internally driven (time) variables, we studied a navigation task that featured two sets of behaviorally important location categories with three elements each. This allowed us to study the neural code for time and space both within and across categories. By analyzing the simultaneous activity of large numbers of mPFC neurons recorded using chronically implanted Neuropixels probes[18], we found that (1) time codes in both location categories generalized to different locations within each category, and (2) a subset of prefrontal neurons was functionally specialized to represent spatial locations or time, as these neurons preferentially represented the same variable across category boundaries. Furthermore, we found that high firing rate cells were particularly important for space and time coding, and that spatial representations of starts and goals were structured so that they reflected the layout of the maze. These results demonstrate how PFC activity is organized to provide structured spatial and temporal information important for solving complex behavioral tasks.

RESULTS

Time, space, and category representations in mPFC

In our delayed match-to-sample (multi-start/multi-goal/multi-route, i.e. "MSMGMR") working memory task[19], rats navigated from one of three start locations to one of three memorized goal locations using variable, unpredictable routes (Fig. 1A). During the sample phase of each trial animals were visually guided to the current goal location (pseudo-randomly assigned) and had to maintain that location in memory while it searched for one of three pseudo-randomly assigned start locations. Once found, the animal had to nose-poke for 3 (or 3.2 s in one animal) at this start location. During this time the animal was unaware which route would become available and thus could not plan its motor actions until the end of the delay period (Fig. 1A). At the end of the delay, a route was made available and, during this test phase of the trial, the animal needed to navigate to the correct goal location in order to obtain reward. In the next trial, the goal and start locations were again pseudo-randomly assigned. Using chronically implanted Neuropixels probes, we sampled a large number of mPFC neurons during task performance.

The goal and start locations are the most important locations in the task and the behavior at these locations is well-controlled; thus, we focused our analysis of spatial and temporal representations on the delay periods at the three start locations and while the animal was at the three goal locations during the sample phase. During these periods animals were stationary, allowing us to avoid the ambiguity of neural representations during locomotion where space and time covary. These periods therefore are ideally suited to directly address single neuron and population-level interactions between space and time representations while the animal is at different locations belonging to two different behavioral categories – starts and goals.

Spatial selectivity in mPFC has been described in open field settings and simple mazes[1,2,20,21]. In our maze, each of the six locations, as well as the location category they belong to, could be decoded from neural

activity with high accuracy (Fig. 1B,C) (six recording sessions from 3 animals, 2 sessions per animal). The mean firing rate of an individual cell could differ for each individual location within one category or one location could be different from two others (Fig. 1B, right), in which case the location with the distinct firing rate could be either higher or lower than the firing rate for the other two locations within the category (Fig. 1B, right, Suppl. Fig. 1).

Neurons in PFC have also been shown to reflect elapsed time in a variety of circumstances[3,7,22,23]. Elapsed time at each of the locations in our task, i.e. after the beginning the nose poke that defines the delay period (3 or 3.2 s) at the start, and in the 3 s period after animals arrived at the goal, could be decoded with a population decoder well above chance (Fig. 1D).

We previously reported that neural activity at different locations clustered according to their meaning in our task ([19], Fig. 1C) and hypothesized that such representations of categories are important for animals to understand and solve the behavioral task. Goal and start location categories can be perfectly decoded from neural activity in all sessions (Fig. 1C, right). Among all cells that were not spatially selective for any individual goal or start location, 74% were selective for category (range over sessions: 60.9% - 87.5%, mean: 75.8%, Suppl. Fig. 2).

Having established that both time and space are represented in both location categories, we asked how time and space codes for individual locations related to one another within and across location categories and whether prefrontal neurons had a functional preference for representing space or time. For instance, regarding the latter, is a neuron that is spatially selective for start locations more likely to be also spatially selective for goal locations?

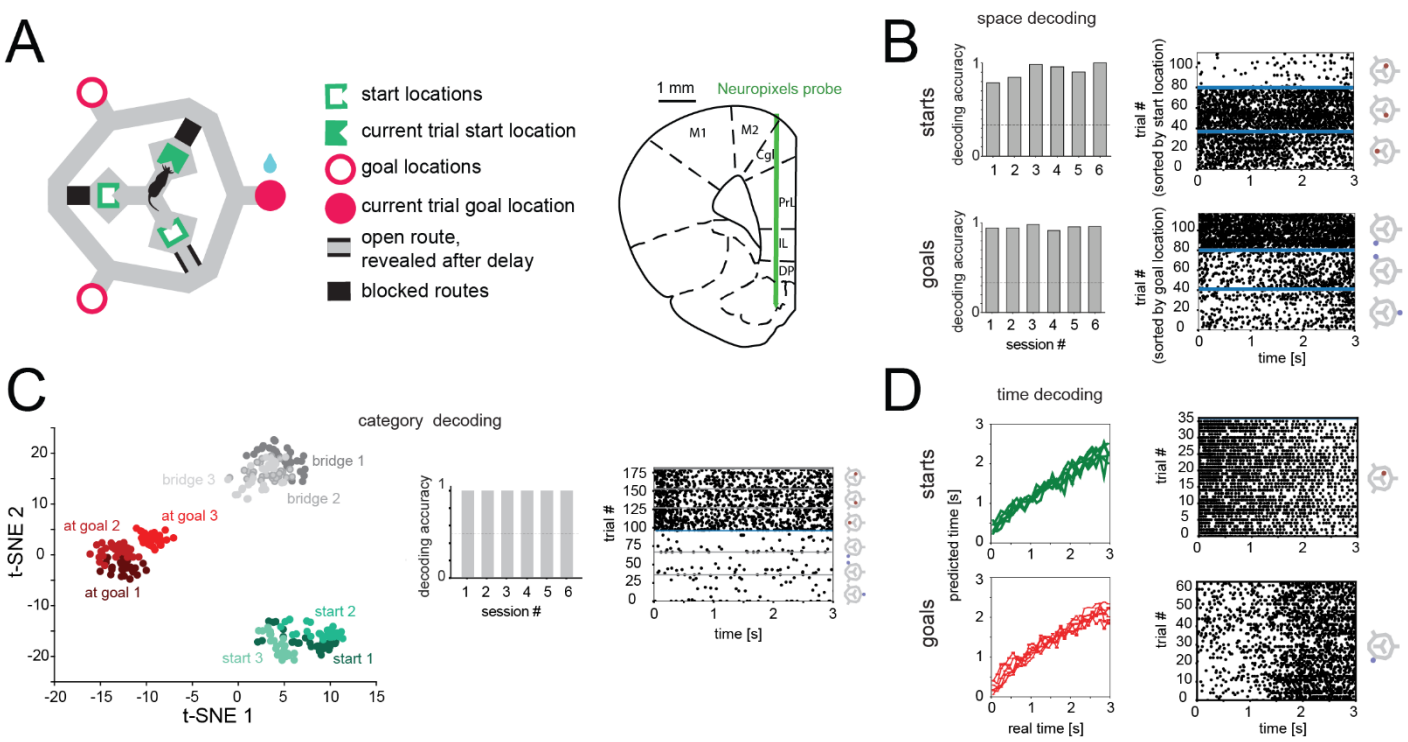

***Figure 1. Space, time and category are represented in prefrontal cortex at key task locations, A**, task layout (left) with two location categories (starts, green; goals, red) and recording location (right), **B**, individual start and goal locations can be decoded from neural activity (chance, dotted line), **C**, neural activity of locations is organized according to their category that is defined by their meaning in the task (left), as shown by the ability to distinguish starts from goals (right), **D**, time can be decoded at starts and goals (time bins 100 ms and 106.7 ms, i.e. 30 bins for the 3 or 3.2 s delay period at starts, for two sessions). Rasters show example neurons with the indicated selectivity.*

A generalized time code in mPFC

First, to visualize the relationship between neural activity at the six different locations at different time points while the animal was stationary, we used principal component analysis (PCA) of the average population vectors at these locations (Fig. 2A, Suppl. Fig. 3). The variance explained by the first principal component was on average 5.5 times higher (range: 3.1 to 7.5, Fig. 2) than the second principal component and appeared to largely represent the overall difference between neural activity at start versus goal locations, consistent with previous analysis using t-SNE. Thus, we performed PCA separately for goal and start locations to visualize the relationship between spatial and temporal components (Fig. 2B and Suppl. Fig. 3). Here, the temporal trajectories were separate for each location and had a common shape and unfolded in parallel for the separate locations. This points to a common, generalized representation of time at different start and goal locations, respectively.

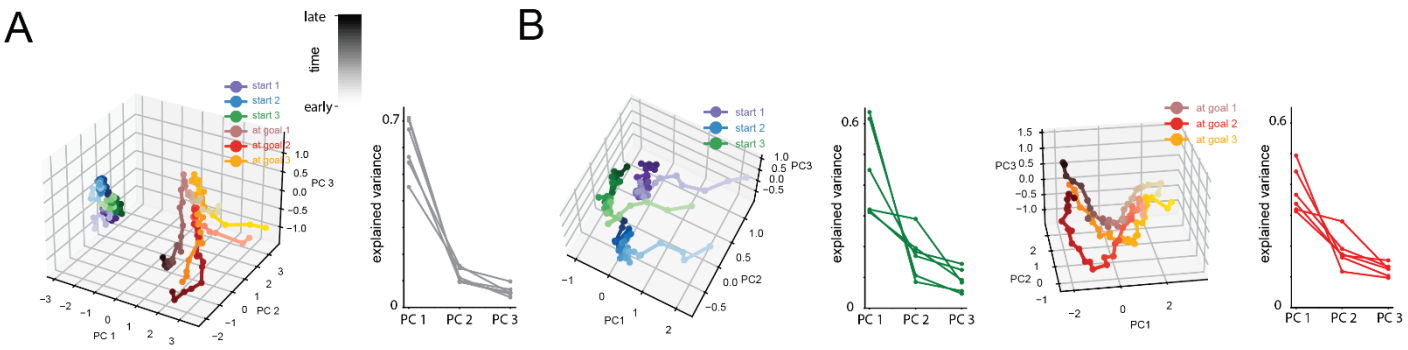

***Figure 2. Parallel trajectories of elapsed time in neural space**, **A**, Principal component analysis (PCA) of mPFC population activity for one session (averaged over trials) at all six locations (goals and starts) together, time bins 100 ms, right: variance explained by the first three PCs for all sessions, **B**, PCA and explained variance for start (left) and at goal (right) locations separately, time evolves in parallel for different locations and primarily along one principal component. Color shades from light to dark correspond to early to late time points at the starts/goals (as indicated in grayscale in A, top).*

We tested this hypothesis of a common time representation directly by training neural population decoders to decode time using any combination of two locations within a category and testing their performance on the respective third location. For this we used binary logistic regression decoders that were trained on the neural data of any combination of two time bins (Fig. 3A). Decoder accuracy of which of the two times bin the data was from was close to perfect for time bins temporally furthest apart and lower for time bins closer in time. Thus, prefrontal cortex activity contains a common code across different locations within each category (goal or start) that reflects elapsed time. To test if the temporal code was partially or fully generalizable to different locations, we compared the precision at which we could decode elapsed time (considering all possible time bins together) with decoders trained with data pooled from all locations in one category or using separate locations for training and test data (cross-location), as above (Fig. 3B). The mean time prediction error was not significantly different for pooled or cross-location decoding for either goals or starts when corrected for multiple comparisons (Fig. 3C). From these results we conclude that the time code is transferrable with minimal precision loss to different locations within a category. Furthermore, while the mean prediction error was proportional to elapsed time at the goal, as expected, there was a consistent dip in mean prediction error between 2 and ~2.7 sec for the delay. This improvement in accuracy could be caused by motor preparation at the upcoming end of the delay period and a concurrent reduction in variance in neural dynamics as animals prepare to run.

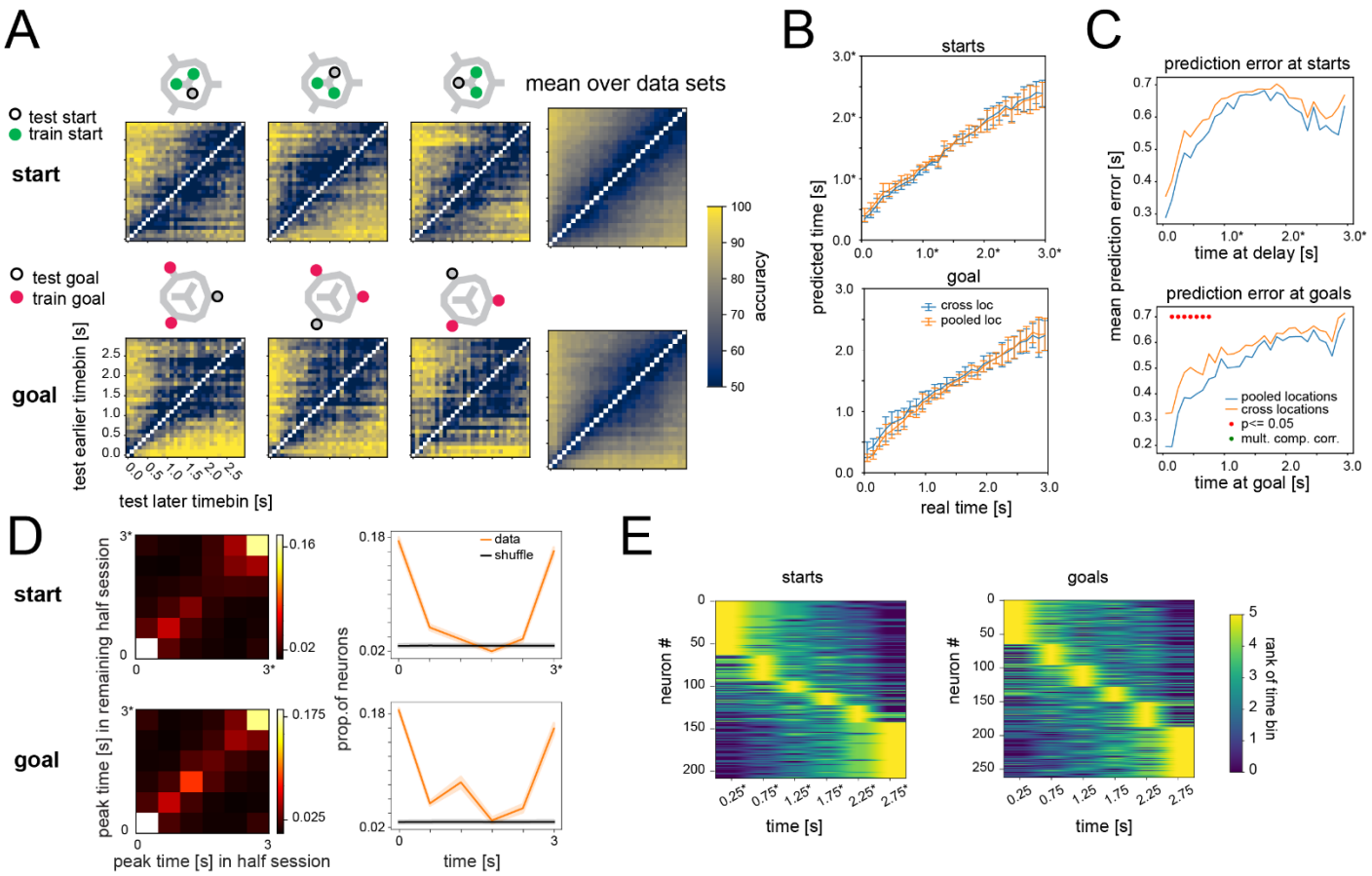

***Figure 3. A generalized time code in prefrontal cortex, A**, binary classification of which of two time bins neural data comes from for all possible time differences for starts (top) and goals (bottom), maze symbols indicate training and test locations. The results below the diagonal correspond to prediction accuracy of the earlier of the two time bins, above the diagonal to the prediction accuracy of the later time bin, **B**, time decoding using all time bins, error bars are standard deviation (std) across sessions, **C**, prediction error (of decoding using all time bins), **D**, consistent activity peaks are primarily at the beginning and at the end of the analyzed time periods, left, comparison of activity peak when dividing dataset in halves, right, proportion of cells with a consistent activity peak at indicated time points (diagonal of matrices on the left, see text for details), **E**, cells ramp up or down at starts and goals, color indicates for each cell the order (rank) of mean firing in each time bin (only cells with consistent peaks are shown, cells are ordered by the peak firing time bin). Displays show pooled results across all data sets for D and E. Time bins are 100 ms (and *106.7 ms for two of six sessions at starts) for A – C and 500 ms (and 533.3 ms for two of six sessions) for D and E.*

What might underlie the firing patterns that differentiate time points at a single-cell level? One possibility that has been described before in parietal cortex and other brain areas is that the delay period is tiled by neurons with firing peaks at different time points[24]. We used a previously described method[25] to determine if cells had consistent firing peaks (Fig. 3D). Specifically, we repeatedly randomly divided each data set into halves and determined the peak of firing in the first half and compared it to the timing of the peak found in the second half. Most cells with consistent firing peaks peaked at the beginning or at the end of the considered time period at starts and goals. These cells tend to increase or decrease their firing gradually (Fig. 3E), consistent with a time code that is primarily generated by cells' firing ramping up or down.

Next, we tested whether the time code was transferrable across goal and start categories. Results differed for different sessions, in one case the time codes for goals and starts overlapped partially, in two cases they were partially reversed, and in the remaining three sessions we saw no evidence for cross-category time decoding (Suppl. Fig. 4). The time codes are thus not, or only partially, consistent for goal and start locations.

The corresponding analysis in the spatial domain, training a decoder to predict spatial locations from one category (e.g. start locations) and testing on spatial locations from the other category (e.g. goal locations), should yield random predictions for the test category if, as expected, spatial codes for start and goal locations were unrelated. Instead, we found an unexpected reflection of the spatial layout of the task: the goal location

opposite the start location in the training set was predicted far below chance in all sessions (Fig. 4A, Suppl. Fig. 5A,B for the reverse analysis, i.e. train on goal data and test on start data, and for single session results). Thus, the classifier axes dividing the start locations in neural activity space divide the respective goal locations into opposite and adjacent goals. This points towards more similar population vectors between goal and start locations that are not located opposite of one another. We tested this directly by correlating the population vectors at start and goal locations with one another (Fig. 4B, Suppl. Fig. 5C). Indeed, correlations were generally negative if the start and goal locations were opposite of one another, and positive or uncorrelated if they were adjacent. We found similar results when we correlated the weights from classifiers trained separately on start and goal locations (Suppl. Fig. 5D). These results demonstrate an unexpected relationship between location codes for behaviorally meaningful categories that is defined by their relative location in physical space. One possible explanation for the relationship between opposite and adjacent start and goal locations could be their direct physical distance in space. This distance was larger between a start and its opposite goal location than between a start and its two adjacent goal locations. However, there were no direct connections between these locations in our elevated maze and the distance an animal traversed from a start to the opposite goal could also be shorter than to an adjacent goal depending on the available bridge in a given trial. Other possibilities could be similar visual inputs or the influence of head-direction tuning. The animal's head direction is 60 degrees offset for the goals adjacent to a start and 180 degrees for a start's opposite goal location. Thus, cells with broad, unidirectional tuning could contribute to our finding that start and goal location codes are related.

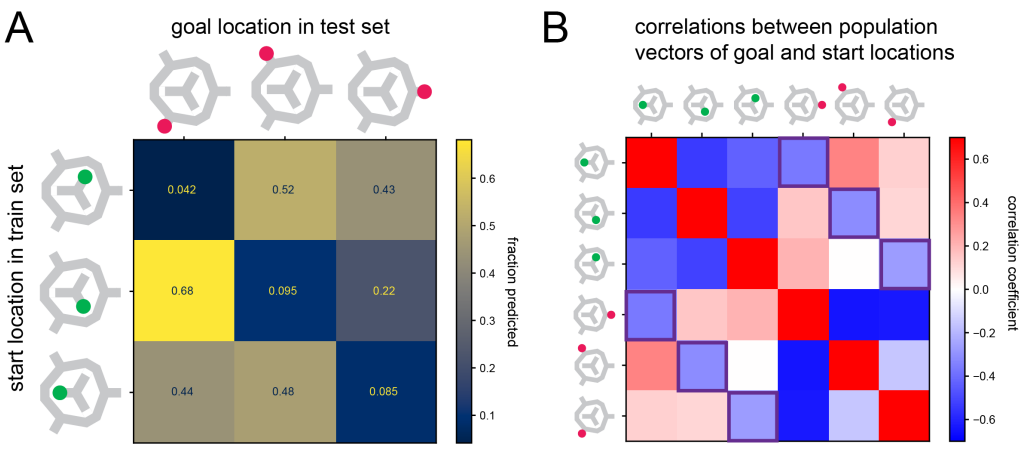

***Figure 4. Spatial codes across categories are structured, A**, predicting goal location with a classifier trained on start locations. Opposite locations were rarely predicted, mean over sessions. **B**, correlation coefficients of population vectors of start and goal locations (the goal location and start location population vectors of all trials were standardized separately before correlation to reveal any structure beyond the high similarity among start and goal location population vectors, respectively). Mean across all 6 sessions. The squares with dark edges denote values corresponding to opposite start and goal locations, mean over sessions.*

Functional specialization in mPFC

The structured relationship between the spatial codes for starts and goals suggests that an overlapping set of cells are responsible for decoding start and goal locations. We thus sought to test for functional preference for spatial location coding – that is, whether a cell had a preference to code for space for both start and goal categories. To do this, we ranked neurons by their impact on classifying goal locations, i.e. we sorted them according to the highest absolute classifier weight for any of the three goal locations. We then consecutively added neurons with decreasing goal classification importance (i.e. decreasing absolute weight) to classifiers for decoding start location. Naturally, the ability to decode start locations improved with more neurons (Fig. 5A). Importantly, decoder performance for start locations improved more steeply when adding neurons ordered by goal decoder classifier weights as compared to randomly selected neurons (Fig. 5A), demonstrating that an overlapping set of neurons is engaged in decoding both start and goal locations. To assess if firing rate could explain this finding, we compared this curve to the improvement of start decoder

performance when adding neurons ranked by their firing rate (high to low, i.e. including higher firing rate neurons first). Firing rate did not account for the steep improvement in performance we observed for neurons selected by classifier weights, though higher firing rate neurons did outperform randomly selected neurons. Results for the reverse analysis, i.e. selecting neurons based on classifier weights for start decoding and probing their impact on goal location decoding, were similar (Fig. 5B). Thus, subsets of neurons are specialized for decoding spatial location across behaviorally important spatial categories.

Taking a similar approach to determine if cells had a functional preference for time, we consecutively added neurons ordered by their classifier weight from a decoder trained to decode time at the goal or start locations, respectively (Fig. 5C,D). Our results indicate that neurons added based on decoder weights did improve decoding accuracy faster than randomly selecting neurons. However, selecting neurons based on firing rate (high to low) was better for improving decoder performance only for low neuron numbers and similarly effective in improving decoder performance for higher numbers. Thus, time decoding at both goals and starts was preferentially supported by higher firing rate cells but, unlike for space, not as strongly by a specific preference for time decoding across different categories independent of firing rate.

We also assessed individual neurons' decoding potential across space and time (i.e. selecting neurons based on classifier weights from a space decoder to decode time and vice versa Fig. 5A-D). The improvement in decoding accuracy when adding neurons ranked by classifier weights of the respective other variable was no different than for randomly ranked neurons. This suggests that preference to decode time and space overlapped no more than expected by chance, but also no less – i.e. preference for time or space was not exclusive.

Ranking neurons by firing rate generally yielded a steeper improvement in decoding accuracy than randomly ordered neurons or using classifier weights from the respective other variable, thus high firing rate was a common predictor of high decoding power for both space and time. We tested if the high firing rate cells tended to be important because of a potentially higher signal to noise ratio, or because these cells were more potent predictors per se. We thus reduced the number of spikes of these neurons by downsampling the number of spikes to match the firing rate of randomly drawn neurons (see methods for details). The resulting decoding accuracy curve was lower than or similar to that of randomly ordered neurons, suggesting that the firing rate itself was responsible for this effect and not another property of these cells (Fig. 5 A-D).

Taken together, these results reveal an organization in which mPFC neurons maintain their functional preference across category boundaries, most prominently for spatial coding.

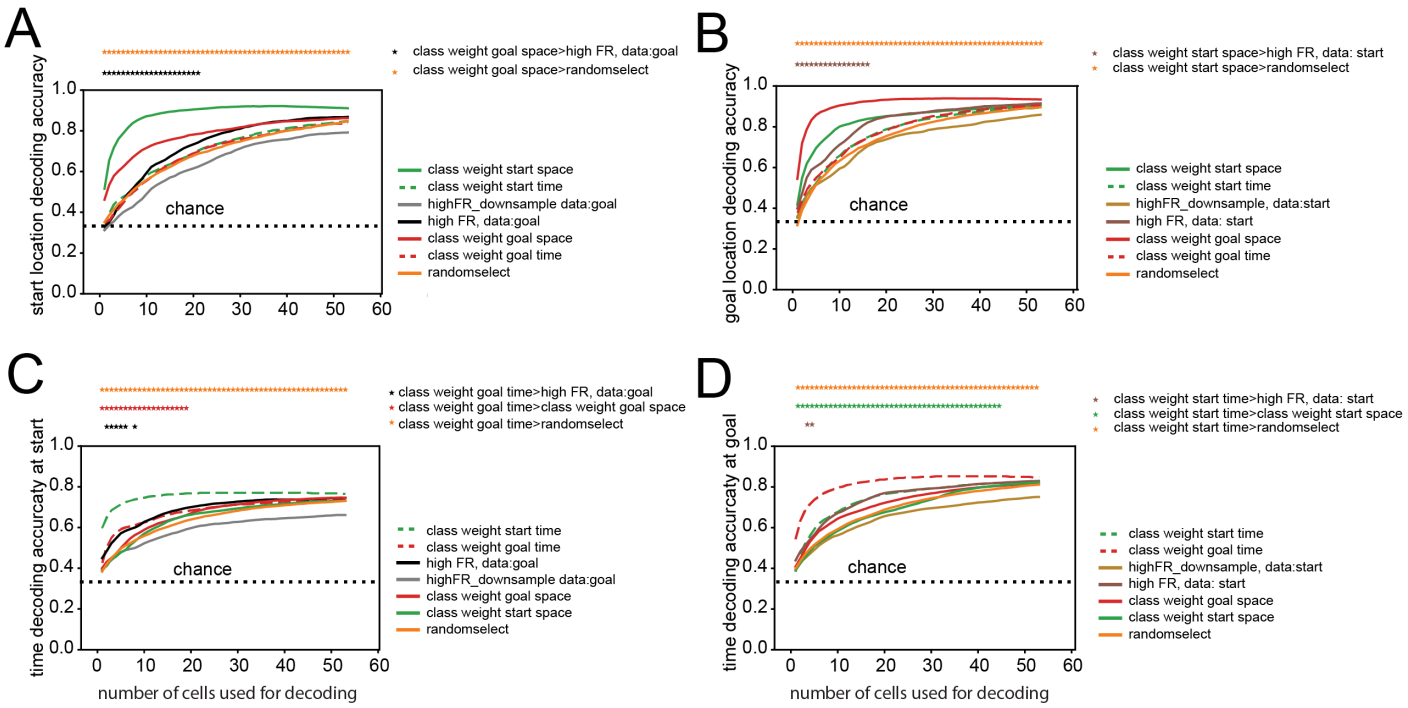

Figure 5. Functional preference of neurons for decoding of space and time across categories. *Decoding accuracy for space (**A**, start, **B**, goal) and time (**C**, at start, **D**, at goal) for increasing numbers of neurons. The order in which neurons were added to the respective decoder was based on classifier weights for space (solid green, start, solid red, goal) or time (dashed green, time at starts, dashed red, time at goals), or firing rate (at goal, black, at start, brown), or averaged down sampled firing rate (gray, at goal, light brown, at start). The orange line is the averaged decoding accuracy for 50 randomly chosen neuron orderings. For space decoding (**A** and **B**) the summed spike count during the full delay period at the start or a 3 sec period at the goal for each trial were used for classification. For time decoding (**C** and **D**), the analyzed time period at the starts and at the goals were divided into 3 time bins. Accuracy was determined as a binary decision. Stars above each plot denote multiple comparison-corrected significance.*

Next, we tested whether neurons from subareas of the mPFC were differentially involved in decoding spatial or temporal variables. We thus compared the distribution of classifier weights from time or space classifiers and tested if there was any bias that could be explained by the recording location (Suppl. Fig. 6). We did not find any consistent differences in anterior cingulate cortex, prelimbic or infralimbic cortex or dorsal peduncular cortex for time or space (see methods for details). However, it should be noted that the precision of our anatomical evaluation of the recording locations was limited, and results for other methods and variables can lead to different results[26].

Our analyses of (population) decoding properties of mPFC neurons do not directly address their individual encoding properties. For instance, two neurons can, theoretically, have the same tuning and thus their contribution would be redundant (and thus missed for one of the cells) in a population-based decoder. To test how individual neurons encode spatial and temporal variables, we used linear-nonlinear-Poisson models previously introduced to characterize encoding properties of medial entorhinal cortex cells[27]. We used this method to predict the spiking activity of each neuron during the delay (at start locations) or, separately, at the goal based on three temporal and spatial predictors each. We binned spiking activity in 3 time bins at each start or goal location, so that for each response one spatial and one temporal predictor out of the total of 6 predictors were nonzero (Fig. 6). For each cell, we tested if a model that included only the spatial or only the temporal predictors was significantly better than a mean firing rate model.

Out of 520 neurons in total, we found 127 (24.4%) were significantly modulated by spatial predictors at starts and 178 (34.2%) at goals. The expected number of cells modulated by both starts and goals if spatial selectivity at starts and goals were independent of one another would be 43.5 (8%). Instead, 74 cells (14.2 %) had both types of spatial selectivity, demonstrating a functional preference for encoding space in a subset

of cells, consistent with the decoding results. Similarly, for time encoding cells, we found 195 (37.5%) and 225 (43.4%) cells at starts and goals, respectively. The expected number of selective cells for time at both categories was 84.4 (16.2%), but we found significantly more, 116 (22.3%). Are cells that encode space in one location category more or less likely to also encode time at that location category? The number of cells we observed that encoded both space and time was similar to the number expected by the fractions encoding each variable independently (at starts, expected: 47.6, 9.2%, observed: 54, 10.4%, at goals, expected: 77.0, 14.8%, observed: 83, 16%). Thus, the subsets of cells that encode space and time do overlap, but not more than expected by their independent incidence. In our previous analysis we identified firing rate as an important factor for decoding space and even more so for time. In line with the decoding results, the average firing rate of neurons that encoded spatial locations (time) at starts or goals was 4.12 Hz (4.40 Hz), higher than the average firing rate of all neurons at starts and goals, 2.75 Hz.

Taken together, in agreement with our population level decoding results, we show here that individual cells that encoded spatial location at starts and goals overlap more strongly than what would be expected from their incidence at starts and goals separately. Similarly, more time encoding cells were found to encode time across category boundaries than expected. However, space and time encoding was not exclusive but instead, within a behavioral category we found cells that encoded both space and time at numbers similar to those expected from their independent incidence These results provide further evidence that prefrontal cortex neurons have functional preferences in general, i.e. across category boundaries.

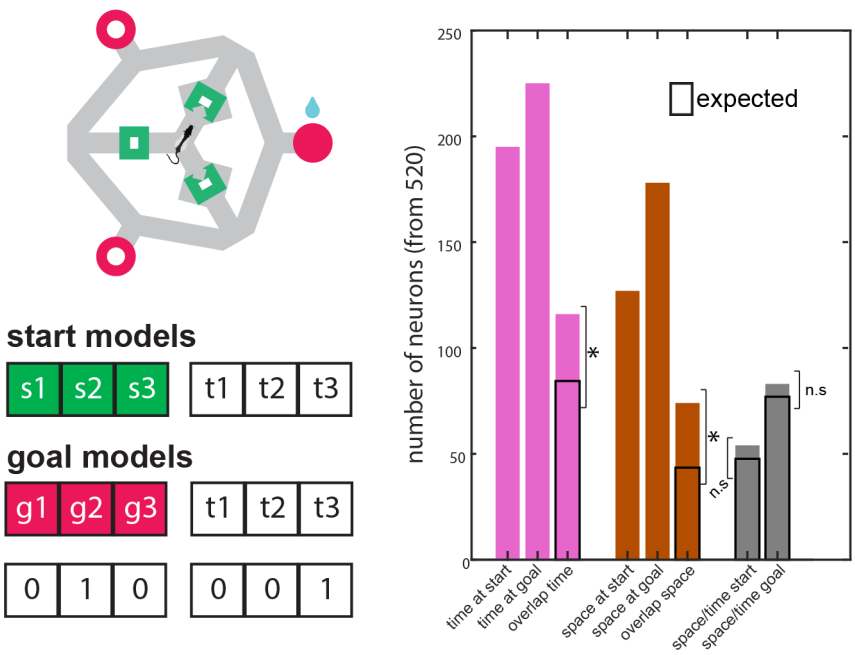

Figure 6. Generalized linear models for predicting individual neuron spiking from spatial and temporal variables at starts and goals. *Left, separate LN models for goal and start locations with 3 spatial and 3 temporal predictors each. Bottom, example of binarized predictors for goal location 2, time bin 3. Right, number of cells that are significantly modulated by time (pink bars) or space (brown bars) at starts or goals. Gray bars, cells significantly encoding both time and space. Overlayed black framed bars: expected number of cells based on fractions of cells selective for each feature (assuming independence). * p<=0.01*

DISCUSSION

The central role of frontal cortices in goal-directed, cognitively demanding tasks is well-accepted; in working memory tasks, prefrontal cortex is required for all phases of the task[28]. A multitude of neural correlates of task-related variables that presumably enable prefrontal cortex function have been described. The high number of correlates often found in single neurons raises the question of whether individual neurons obey any principles of structural or functional organization. It has also been suggested that some functional

aspects could arise only at the population level[11]. We focused here on correlates of time and space in relation to a third, higher-order variable, location category, to probe structural organization.

We recorded a large number of neurons using chronic Neuropixels probe recordings in freely moving rats performing a richly featured behavioral task. In particular, categorization is a key aspect of PFC representations[8,10], and our task allowed us to dissect the neural correlates of the fundamental variables of space and time within and across behaviorally relevant category boundaries. We found that the code for elapsed time in prefrontal cortex is flexibly transferrable to different locations within location categories (i.e. starts or goals). This shows that, while prefrontal cortex neurons are often selective for multiple variables, behaviorally important variables can be independent of one another (i.e. the value of one does not necessarily influence the other), which constitutes an efficient coding principle. Furthermore, by testing whether individual neurons consistently exhibited selectivity for space or time across different location categories, we found that particular neurons do have functional preferences for space or time.

While we found that the time code is transferable within one location category, a largely different code is used for the respective other category, even though an overlapping set of neurons is used for both categories. The delay period (at starts) is a fixed time interval, while goal timing is tied to the onset of a behavioral event (i.e. arrival at the goal) and – as indicated by the different shapes of prediction error curves (Fig. 3C) – other factors than elapsed time are likely to impact neural dynamics. Furthermore, rats received a reward at the goal, but not during the delay period. These differences between goal and start locations might have thus concealed a common time code in our analysis, and methods to transform neural activity from one category of locations to another might yield different results. The space codes for the two different location categories, on the other hand, were linked – they reflected the spatial layout in the maze such that the start location codes separated the respective opposite goal location from the adjacent goal locations.

Whether or not individual neurons are organized into functional subclusters has been investigated in other brain areas associated with higher-order cognitive function. In parietal cortex, in a multisensory decision-making task, no such structure was found[29]. We show here that, in mPFC, the time code is independent of spatial location within a category, and that space and time encoding in individual cells did not overlap more than expected by their independent incidence. This is in line with the finding in parietal cortex that choice and modality were independent of one another, and that the same population of neurons could give rise to either pattern. In our task, however, with two spatial categories with three elements each, we could also probe the same neurons under two different conditions. This internal comparison was essential for allowing us to discover that subsets of neurons preferentially encoded time or space. A similar approach has been taken in an economic decision-making task in monkeys[30]. Here, animals were presented with two different sets of choices, and orbitofrontal cortex (OFC) neuron selectivity for economic decision variables was compared across those sets of choices. Neurons maintained their specific selectivity across choice sets and thus formed a stable framework that can adapt to different contexts by 'remapping' their selectivity to the currently relevant choice set. Using unbiased clustering approaches, the organization of single neurons into functional groups has also been revealed in rodent OFC[13,14]. Hirokawa et al.[13] further linked a group of functionally distinct neurons to a specific projection target, suggesting that functional separation might be accompanied by distinct connectivity. In mouse anterior lateral motor cortex (ALM), functional subpopulations were also found and linked to the varying strength of input from other brain areas[15]. A study in MEC specifically investigated selectivity for time and space of individual neurons across visually different environments[31]. In line with our results from mPFC, medial entorhinal cortex (MEC) time and space cells preferentially encoded the same variable across different contexts. In MEC, time and space cells were

organized in anatomical subclusters and associated with different behavioral states (movement and immobility).

Thus, in higher-order brain areas, functional preferences appear to be a common organizational principle. Structural organization into functional subclusters has been proposed to be computationally beneficial or even required for cognitive flexibility, as for example when learning multiple tasks and transferring learned representations from one task to another[16]. In artificial networks trained to perform common neuroscience tasks, those that required flexible input-output mappings displayed non-random population structure[17]. Thus, identification of structure might critically depend on details of the task or environment, such as the availability of different contexts, and how animals were trained.

Future work should examine further characteristics of functional mPFC clusters, such as subsets that are defined by projection targets or molecular markers[13,32–34]. Another area of investigation could be how representations of task-related variables and functional specialization emerges during learning or whether there are factors that predetermine such functional organization. Taken together, using a behavioral task where the relationship between neural correlates of time and space could be studied directly, we identified a distinct functional organization that could modularize functional elements of behavior and may be a hallmark of brain areas involved in higher order cognitive function.

METHODS

Experimental procedures

Details on experimental procedures including surgery, behavior, and histology have been described previously[19]. The data used for the current study are partially overlapping with our previous work where we reported a different set of findings. All procedures were conducted in accordance with the Janelia Research Campus Institutional Animal Care and Use Committee. Briefly, the data presented here was collected from three male Long-Evans rats. From each animal 2 sessions from two days that were 3 to 4 days apart were included (the first but not second session per animal was analyzed in[19]). Single-shank Neuropixels 1.0 probes [18] (https://www.neuropixels.org) were implanted chronically and fixed in place (i.e. not moved in between recording sessions). In each animal, one such Neuropixels probe was implanted in the right hemisphere at 3.24 mm anterior-posterior and 0.6 mm medio-lateral, at a depth of 6 or 6.2 mm. The recording sites spanned anterior cingulate cortex, prelimibic and infralimbic cortex and, in 2 animals, dorsal peduncular cortex. The probe location was confirmed with standard histological procedures. Recordings were conducted once animals were fully trained in the multi-start/multi-goal/multi-route (MSMGMR) behavioral task. This match-to-sample spatial working memory task was conducted on an elevated maze and consisted of a sample phase and a test phase. In the sample phase, the animal navigated from the center (Fig. 1A) to one of the three goal locations (pseudorandomly chosen in each trial and visually marked to guide the animal) via the available bridge (out of three total bridges, which were movable elements in the elevated maze that connected the outer ring and goals with the center; the available bridge in the sample phase was chosen pseudorandomly). Once the goal was reached, a small liquid food reward (Ensure Plus) was automatically delivered. The delivery was triggered by the animal breaking an infrared beam at the reward pod. Next, the animal returned to the center, received another small reward, then had to search for the one location of the three start locations (Fig. 1A, green rectangular shapes) that was pseudorandomly chosen in each trial. Each of the start locations was equipped with a nose poke port, and the correct nose poke (i.e. the nose poke at the start chosen for that trial) was indicated by a tone emitted from the port while being poked. The nose poke duration ('delay period') was 3 s in two animals and 3.2 s in the third animal. During this period, all bridges were lowered, i.e. the animal had no access to the outer ring of the maze. Which bridge would eventually be accessible was not known to the animal and thus the animal could not plan or prepare the route it would have to take during the delay period. After the delay period at one of the start locations, a pseudorandomly chosen bridge became available and the test phase began. In the test phase the rat had to navigate, without any external cues, to the goal location that was rewarded in the sample phase. If the animal chose the correct goal location, it received a reward, then it returned to the center and the sample phase of the next trial began.

Neural data was recorded and stored using SpikeGLX software (http://billkarsh.github.io/SpikeGLX/). The spike data was first automatically presorted and then manually curated using the JRCLUST software package[35]. We isolated on average 142.8 neurons per session (range: 98 - 182) across prefrontal cortex subareas. Only cells that were stable over the recording session, selected based on the previously described methods[19], were used for the analyses shown in this study. After also excluding presumptive interneurons, the number of neurons analyzed was on average 86.6 neurons per session (range: 68 - 99), 520 in total over the 6 sessions. The core analyses were repeated and the results confirmed when including all clusters isolated during spike sorting.

Data Analysis

All analyses were conducted using custom-written code in Python or MATLAB. The analyses presented here were focused on two defined periods during task execution. First, the delay period at any one of the start locations (3 or 3.2 s) and, second, the period after the animal had arrived at any one of the three goal locations. For analyses where the spike data were transformed into a spike rate by splitting the time period into time bins and counting the number of spikes that fell into each bin, the binwidth for all analyses involving the delay period was adjusted to the length of the delay period, so that for all sessions the same number of bins was used. The time period used for analysis at the goal was 3 s, starting from the time point the infrared beam at the reward pod was broken. The reward was triggered by the animals breaking the infrared beam at the reward pod. The animal was free to leave any time but generally remained at the reward site to consume the reward for at least 3 s. As this also matched the delay period duration, we chose to analyze neural activity in this 3 s time window at the goals. To reduce variability in the time period at the goal, we only used data from the sample phase. (We had previously shown that the activity at any one goal location during sample and test phases is distinguishable but overlapping and distinct from that at any other goal location during test and sample phases[19].) For the delay period at the start locations, we used trials where in the following test phase the animal made a correct or incorrect choice. For the goal periods we used only trials where the animal chose the correct, visually indicated goal location and disregarded the outcome of the following test phase.

For all of the time or space decoding analyses we used multinominal logistic regression classifiers with L2 penalty. Results were comparable using other methods, such as support vector machines (SVM) or, for time, using linear regression with continuous response variables. For time decoding, we used a variable number of time bins, as indicated in the Results text or figure legends.

To analyze details of spatial selectivity (Suppl. Fig. 1) we first determined for each data set the cells that had different firing rates at the three different locations within a category using the Kruskal-Wallis test. We then used pairwise post hoc comparisons (Conover's test) to determine which pairs were different and compared the firing rates of those that were different. In Suppl. Fig. 2 we addressed whether neurons can have selectivity for a category of locations without individual location selectivity. Thus, for cells without selectivity for individual goal or start locations, we tested whether they distinguished between starts and goals (Kruskal-Wallis test).

For the principal component analysis in Fig. 2 and Suppl. Fig. 3, the data at the starts and at the goals were binned into 30 equally sized time bins, averaged over trials for each location, and centered.

To test if the time code was transferrable to different locations (Fig. 3A), we trained a decoder on two locations of one location category (starts or goals) and tested its performance on the third location of that category. Each combination of two time bins was trained and tested separately. For example, a classifier was trained on goal locations 1 and 2, time bin 1 and time bin 10 (30 time bins of size 100 ms, or 106.7 ms for the 2 sessions during the delay where the delay period was 3.2 s for one animal), and then tested on time bins 1 and 10 on data from goal location 3. The upper and lower half of the matrix in Fig. 3A are the prediction accuracies for the earlier or later of the two time bins, respectively. The diagonal would not be a valid comparison (one class only) and is thus not filled. All possible combinations of two time bins for all possible combinations of two training location and one test location were analyzed in this way.

When we determined prediction accuracy over all time bins (Fig. 1D, Fig. 3B) we used three approaches. First, only data from one start or one goal location was used (Fig. 1D). Second, data from all locations of one

category were pooled. In these two cases we trained on all trials, except for one which was used for cross-validated testing. The procedure was repeated for all test trials. Third, we trained using data from two locations and tested on the third (Fig. 3B). We repeated this procedure for all three possible combinations of two training locations and one test location for each category. Because here the test set was separate from the train set by design, we did not perform leave-one-trial-out testing but instead evaluated all test trials on the same trained model. For all approaches the mean predictions were obtained by taking the average across the predictions across all trials for each time bin. To assess differences in mean prediction error (Fig. 3C) we calculated the error (the absolute difference between predicted and true time) for all trials from all sessions and tested each time bin separately using the two-sample Kolmogorov-Smirnov test. P-values were based on two-sided tests and corrected for multiple comparisons using the Holm-Sidak method.

For time predictions across categories (Suppl. Fig. 4), we trained a logistic regression classifier on all trials from one location category, i.e. all three start locations, and tested on all locations of the other category. We split the time period at the three start locations and at the three goal locations into three time bins. All data were standardized together, i.e. all time bins from both location categories were concatenated, the resulting mean was subtracted, and each time was divided by the standard deviation. We also tested different forms of standardization: standardizing data from each category separately, or determining the mean and standard deviation from one category and applying the parameters to the other category. The results varied slightly for single sessions across these methods, but none of these standardization methods reliably facilitated time decoding across category boundaries for all sessions.

To test if the underlying neural code for time was based on sequential firing, we employed a modified version of a previously described method[25]. For each session, the data at the goal or at the start was binned into six time bins and a random half of all trials was averaged. For each cell the time bin with the highest firing rate was found. Next, the other half of trials was averaged and again the time bin with the peak firing rate was determined for each cell. This procedure was repeated 1000 times and the proportion of neurons whose peak firing fell into the same time bin for both splits was determined. If there was more than one time bin with the same firing rate, one of them was chosen at random. As a control, we shuffled the time bins in all trials (1000 times) and performed the same procedure (Fig. 3D). As the majority of cells with consistent firing peaks were active at the beginning or the end of the analyzed period, we tested whether cells tended to ramp up or down, i.e. gradually changed the firing rate, which could serve as the basis for the observed time code. We restricted this analysis to cells which fired more consistently than 95% of the shuffled controls. For each cell we then determined the rank with regards to firing rate of each time bin and sorted them according to the time bin with the highest rank (Fig. 3E).

For the cross-location category spatial decoding (Fig. 4, Suppl. Fig. 5) we trained a logistic regression classifier on all trials from one location category (starts or goals). We used the trained classifier to predict locations in the respective other category and found that the predictions were not randomly distributed but biased towards predicting the respective adjacent location. Training a classifier on goal or start locations yielded three weight vectors for both categories, one for each class, with a length equal to the number of neurons recorded in that session. We calculated Pearson's correlation coefficient for the six resulting weight vectors to examine the relationship between start and goal location codes (Suppl. Fig. 5C). For the correlations of population vectors (Fig. 4 and Suppl. Fig. 5C), we first standardized the data at goals and starts separately by subtracting the mean and dividing by the standard deviation. We then took the mean at each of the six locations resulting in 6 vectors and calculated Pearson's correlation coefficient.

Functional specialization

To assess whether neurons were functionally specialized, we compared the accuracy of logistic regression classifiers (for space or time, at starts or at goals) while successively adding neurons sorted according to four different methods (Fig. 5):

- Classifier weights: As a measure for the importance of a particular cell to decode a particular variable, we used the highest absolute classifier weight for any of the classes in a particular type of classifier. Cells were then sorted from highest weight to lowest weight and added in this order to compare the impact on accuracy compared to another order. Four different cell orders were determined in this way, corresponding to the two variables we analyzed (time and space) and the two location categories (starts and goals).

- Random selection: Here, cells were ordered randomly (without replacement)

- Firing rate: For each location category (start and goals), the summed spike count at all starts or at all goals was used to order cells from highest firing rate to lowest firing rate.

- Downsampled firing rate: To match the firing rate of high firing rate neurons to that of randomly selected neurons, we first ordered neurons according to their summed spike count at goals or at starts, respectively, as above. Next, we generated a randomly ordered list of the same neurons. We then matched the firing rate of each cell in the rate-ordered list to that of the neuron in the randomly generated list at the same position. This was achieved by randomly removing as many single spikes as the difference between the two firing rates. If the firing rate of the neuron in the randomly generated list was the same or higher than that in the rate-ordered list, no spikes were removed.

To achieve reliable estimates of the resulting accuracy curves, we used 80% of the neurons available in each session, performed the different sorting procedures with these selected neurons, determined how accuracy improved with an increased number of neurons, then repeated this procedure 50 times and pooled the results from all sessions. We then tested separately each feature size (i.e. the number of neurons included in the classifier) and compared sets of different orders of neurons (e.g. weights for start decoding and random selection) using the Mann-Whitney-Test, the results of which were then corrected for multiple comparisons using the Holm-Sidak method. For Fig. 5, the results from the 50 runs and all six sessions were averaged.

Subareas of prefrontal cortex

To determine whether any of the mPFC subareas we recorded from were more or less involved in coding for time or space, we determined the approximate recording location for each cell with reference to the surface of the brain (Suppl. Fig. 6). We trained classifiers to decode time or space at the start and goal locations (using 3 time bins for time and one time bin for space). The classifier training resulted in weight vectors for each of the classes (locations one to three and time points one to three). The maximum absolute weight for either of the classes for each cell was taken as a measure for its ability to distinguish between the classes for this variable. For visualization in Suppl. Fig. 6, we divided the maximum absolute weight by the sum of all weights of all cells in that session. For the subarea comparison, we again used the maximum absolute weight for either class for each cell and pooled the results for each session for start and goal locations, resulting in

two values for each cell for time and two values for space. The cells were split into groups corresponding to the mPFC subareas. For both variables (space and time) we used the Kruskal-Wallis H-test to determine whether the medians of the groups were equal. In sessions where they were not equal, we further identified the groups that were different using post hoc pairwise tests for multiple comparison (Dunn's test). For space in 3/6 sessions the group medians were different, in one session DP had higher values than all other areas, in another session prelimbic cortex had higher values than ACC and infralimbic cortex, and ACC was significantly higher than infralimbic cortex. In the third session with different group medians, area DP had higher values than prelimbic cortex. For time 2/6 sessions had significant differences in group medians. Post hoc analysis revealed that in one session ACC had significantly higher values than DP and infralimbic cortex. In the other session infralimbic cortex had significantly higher values as compared to DP. It should be noted that DP was only recorded in 4/6 sessions.

GLM analysis

For the encoding analysis (Fig. 6), we used linear-nonlinear-Poisson models previously described in[27]. Data from the goal locations and the start locations were modeled separately, and space and time encoding were determined separately for each cell. A cell was called 'modulated' by a variable if the model was significantly better than the null model (i.e. where the firing rate was set to the same mean rate for all trial types). We tested whether the number of cells that were modulated by time (or space) at both starts and goals were higher than expected by their independent incidence at these location categories empirically: from a pool of numbers as large as the total number of cells (520), we first randomly drew the observed number of selective cells at one location category without replacement and then the observed number of selective cells at the other location category. We repeated this procedure 10000 times and counted how many numbers were identical. p-values were then found by comparison to the real number of cells that were found to be selective for the same variable in both location categories.

Acknowledgements

This work was funded by the Howard Hughes Medical Institute. We thank S. Erwin and R. Gattoni for help with animal training, T. Harris, J. Colonell, B. Karsh and W. Sun for help and advice with Neuropixels probes and software, J. Arnold, S. Sawtelle, P. Polidoro and M. Gugiu for help with setting up the maze, and Sandro Romani and Carsen Stringer for advice on analyses and comments on the manuscript.

REFERENCES

1. Jung, M. W., Qin, Y., McNaughton, B. L. & Barnes, C. A. Firing characteristics of deep layer neurons in prefrontal cortex in rats performing spatial working memory tasks. *Cereb. Cortex N. Y. N 1991* **8**, 437-450-437–450 (1998).

2. Hok, V., Save, E., Lenck-Santini, P. P. & Poucet, B. Coding for spatial goals in the prelimbic/infralimbic area of the rat frontal cortex. *Proc Natl Acad Sci U A* **102**, 4602-4607-4602–4607 (2005).

3. Kim, J., Ghim, J.-W., Lee, J. H. & Jung, M. W. Neural correlates of interval timing in rodent prefrontal cortex. *J. Neurosci. Off. J. Soc. Neurosci.* **33**, 13834-13847-13834–13847 (2013).
4. Xu, M., Zhang, S., Dan, Y. & Poo, M. Representation of interval timing by temporally scalable firing patterns in rat prefrontal cortex. *Proc. Natl. Acad. Sci.* **111**, 480–485 (2014).
5. Wang, J., Narain, D., Hosseini, E. A. & Jazayeri, M. Flexible timing by temporal scaling of cortical responses. *Nat. Neurosci.* **21**, 102–110 (2018).
6. Murray, J. D. *et al.* Stable population coding for working memory coexists with heterogeneous neural dynamics in prefrontal cortex. *Proc. Natl. Acad. Sci.* **114**, 394–399 (2017).
7. Cueva, C. J. *et al.* Low-dimensional dynamics for working memory and time encoding. *Proc. Natl. Acad. Sci.* **117**, 23021–23032 (2020).
8. Freedman, D. J., Riesenhuber, M., Poggio, T. & Miller, E. K. Categorical representation of visual stimuli in the primate prefrontal cortex. *Science* **291**, 312-316-312–316 (2001).
9. Wallis, J. D., Anderson, K. C. & Miller, E. K. Single neurons in prefrontal cortex encode abstract rules. *Nature* **411**, 953-956-953–956 (2001).
10. Reinert, S., Hübener, M., Bonhoeffer, T. & Goltstein, P. M. Mouse prefrontal cortex represents learned rules for categorization. *Nature* 1–7 (2021) doi:10.1038/s41586-021-03452-z.
11. Rigotti, M. *et al.* The importance of mixed selectivity in complex cognitive tasks. *Nature* **497**, 585–590 (2013).
12. Stokes, M. G. *et al.* Dynamic Coding for Cognitive Control in Prefrontal Cortex. *Neuron* **78**, 364–375 (2013).
13. Hirokawa, J., Vaughan, A., Masset, P., Ott, T. & Kepecs, A. Frontal cortex neuron types categorically encode single decision variables. *Nature* **576**, 446–451 (2019).
14. Hocker, D. L., Brody, C. D., Savin, C. & Constantinople, C. M. Subpopulations of neurons in lOFC encode previous and current rewards at time of choice. *eLife* **10**, e70129 (2021).
15. Yang, W., Tipparaju, S. L., Chen, G. & Li, N. Thalamus-driven functional populations in frontal cortex support decision-making. *Nat. Neurosci.* **25**, 1339–1352 (2022).
16. Yang, G. R., Joglekar, M. R., Song, H. F., Newsome, W. T. & Wang, X.-J. Task representations in neural networks trained to perform many cognitive tasks. *Nat. Neurosci.* **22**, 297–306 (2019).

17. Dubreuil, A., Valente, A., Beiran, M., Mastrogiuseppe, F. & Ostojic, S. The role of population structure in computations through neural dynamics. *Nat. Neurosci.* **25**, 783–794 (2022).

18. Jun, J. J. *et al.* Fully integrated silicon probes for high-density recording of neural activity. *Nature* **551**, 232-236-232–236 (2017).

19. Böhm, C. & Lee, A. K. Canonical goal-selective representations are absent from prefrontal cortex in a spatial working memory task requiring behavioral flexibility. *eLife* **9**, (2020).

20. Fujisawa, S., Amarasingham, A., Harrison, M. T. & Buzsáki, G. Behavior-dependent short-term assembly dynamics in the medial prefrontal cortex. *Nat Neurosci* **11**, 823-833-823–833 (2008).

21. Zielinski, M. C., Shin, J. D. & Jadhav, S. P. Coherent Coding of Spatial Position Mediated by Theta Oscillations in the Hippocampus and Prefrontal Cortex. *J. Neurosci.* **39**, 4550–4565 (2019).

22. Bakhurin, K. I. *et al.* Differential Encoding of Time by Prefrontal and Striatal Network Dynamics. *J. Neurosci.* **37**, 854–870 (2017).

23. Tiganj, Z., Jung, M. W., Kim, J. & Howard, M. W. Sequential Firing Codes for Time in Rodent Medial Prefrontal Cortex. *Cereb. Cortex* **27**, 5663–5671 (2017).

24. Harvey, C. D., Coen, P. & Tank, D. W. Choice-specific sequences in parietal cortex during a virtual-navigation decision task. *Nature* **484**, 62-68-62–68 (2012).

25. Inagaki, H. K., Inagaki, M., Romani, S. & Svoboda, K. Low-Dimensional and Monotonic Preparatory Activity in Mouse Anterior Lateral Motor Cortex. *J. Neurosci.* **38**, 4163–4185 (2018).

26. Diehl, G. W. & Redish, A. D. Differential processing of decision information in subregions of rodent medial prefrontal cortex. 2022.08.04.502840 Preprint at https://doi.org/10.1101/2022.08.04.502840 (2022).

27. Hardcastle, K., Maheswaranathan, N., Ganguli, S. & Giocomo, L. M. A Multiplexed, Heterogeneous, and Adaptive Code for Navigation in Medial Entorhinal Cortex. *Neuron* **94**, 375-387.e7 (2017).

28. Vogel, P., Hahn, J., Duvarci, S. & Sigurdsson, T. Prefrontal pyramidal neurons are critical for all phases of working memory. *Cell Rep.* **39**, 110659 (2022).

29. Raposo, D., Kaufman, M. T. & Churchland, A. K. A category-free neural population supports evolving demands during decision-making. *Nat. Neurosci.* **17**, 1784–1792 (2014).

30. Xie, J. & Padoa-Schioppa, C. Neuronal remapping and circuit persistence in economic decisions. *Nat. Neurosci.* **19**, 855–861 (2016).

31. Heys, J. G. & Dombeck, D. A. Evidence for a subcircuit in medial entorhinal cortex representing elapsed time during immobility. *Nat. Neurosci.* **21**, 1574–1582 (2018).

32. Economo, M. N. *et al.* Distinct descending motor cortex pathways and their roles in movement. *Nature* **563**, 79–84 (2018).

33. Cembrowski, M. S. *et al.* Dissociable structural and functional hippocampal outputs via distinct subiculum cell classes. *Cell* **173**, 1280-1292-1280–1292 (2018).

34. Park, J. *et al.* Motor cortical output for skilled forelimb movement is selectively distributed across projection neuron classes. *Sci. Adv.* **8**, eabj5167 (2022).

35. Jun, J. J. *et al.* Real-time spike sorting platform for high-density extracellular probes with ground-truth validation and drift correction. 101030 Preprint at https://doi.org/10.1101/101030 (2017).

SUPPLEMENTARY FIGURES

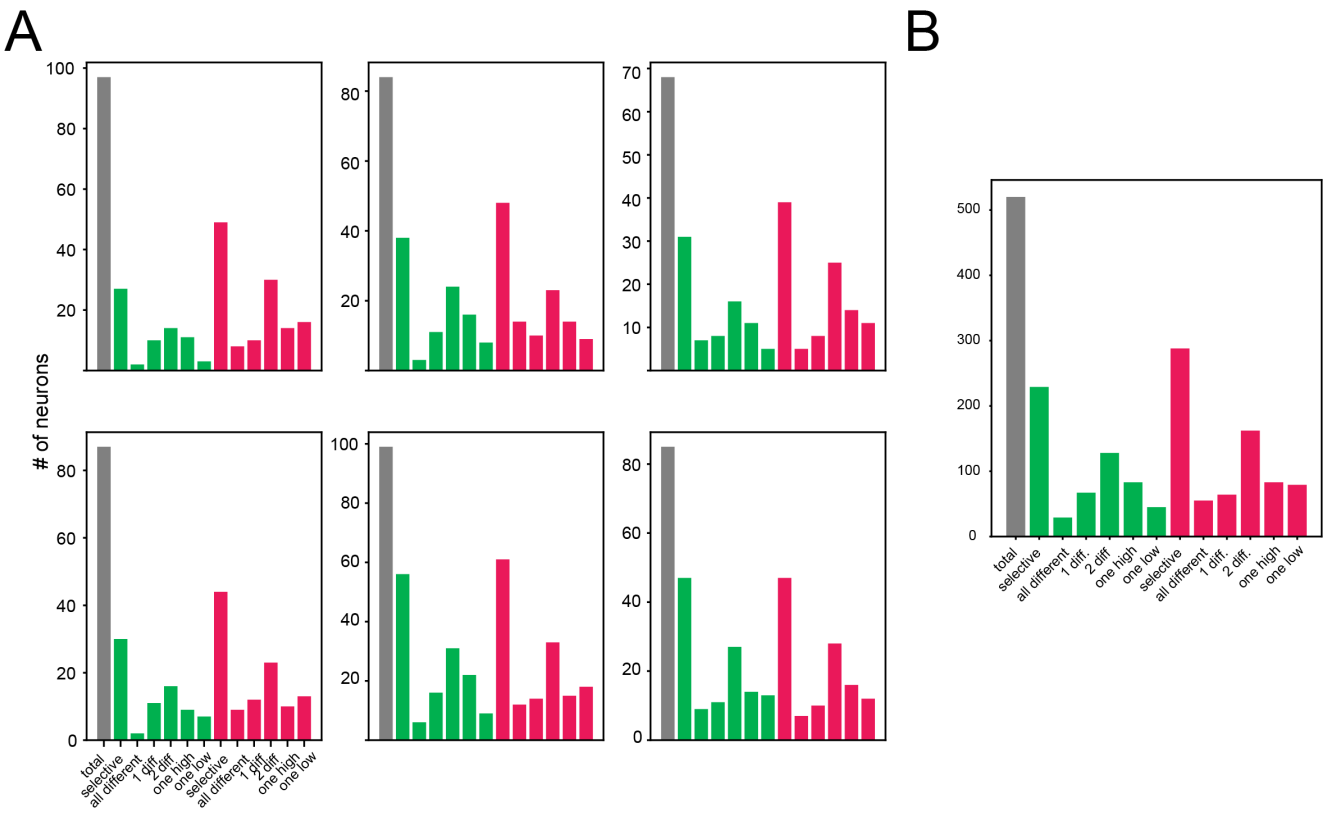

Supplementary Figure 1. Types of spatial selectivity. *Gray: total number of neurons. Green: at starts, red: at goals. Selective: number of neurons that are spatially selective, all selective: number of neurons with differential firing at all three locations, 1 diff: number of neurons where firing at one location is different from that at one other location, 2 diff: number of neurons where firing at one location is different from that at the two other locations, and for these "2 diff" cells the firing rate at the location where it is different can be higher (one high) or lower (one low) than at the two other locations.* ***A****, single session,* ***B,*** *all sessions pooled.*

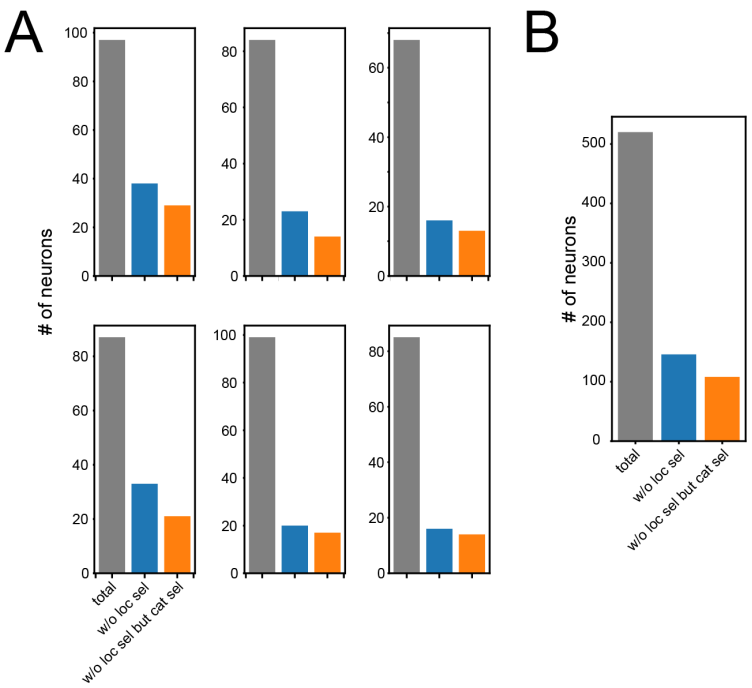

Supplementary Figure 2. Category selective cells without spatial tuning for individual locations. *Gray: total number of cells, blue: number of cells without spatial selectivity for starts or goals, orange: number of these latter cells (in blue) that are selective for category (i.e. their firing rate for starts is different from that for goals.* ***A****, single sessions,* ***B,*** *all sessions pooled.*

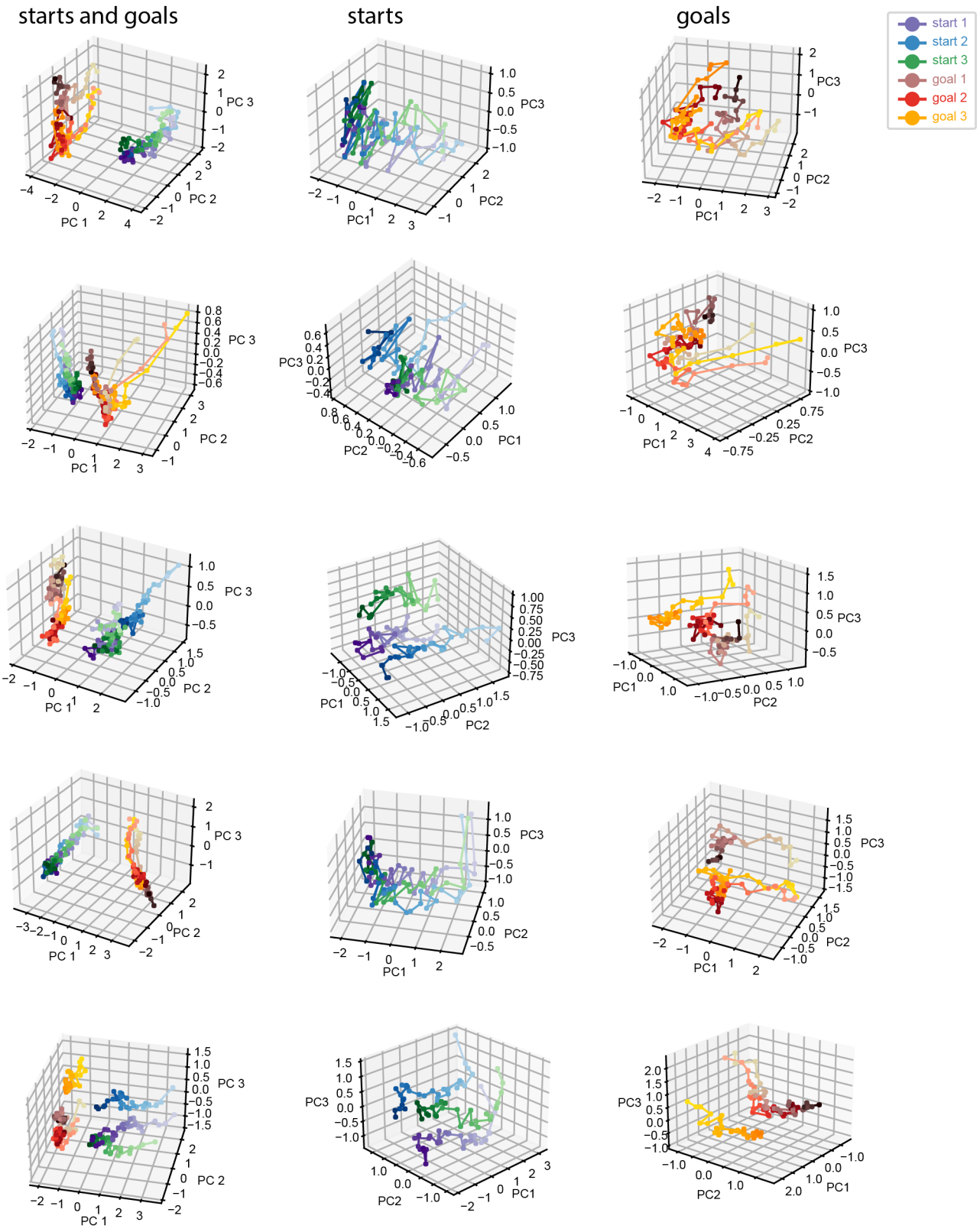

Supplementary Figure 3. Principal component analysis for single sessions*. Left column: PCA of mPFC population activity (averaged over trials) at goals and starts, time bins 100 ms and 106.7 ms for starts in 2 data sets. PCA for start (middle column) and at goal (right column) locations separately: note that time elapses in parallel for different locations and primarily along one principal component. Color shades from light to dark correspond to early to late time points at the starts/goals. Each row corresponds to one recording session.*

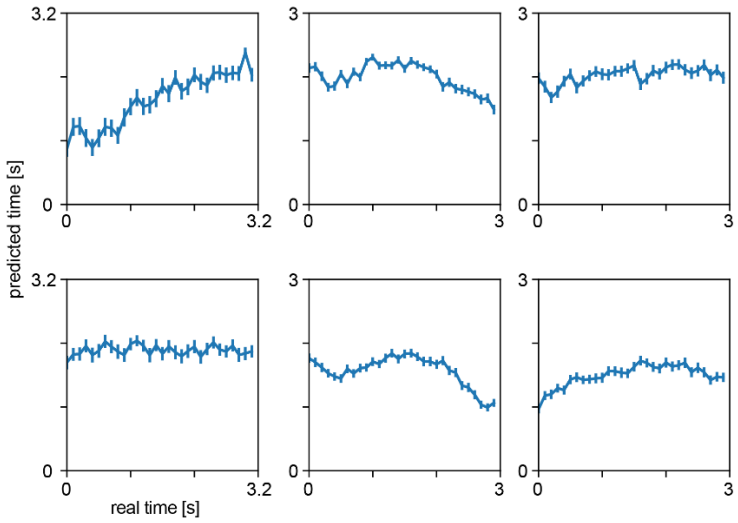

Supplementary Figure 4. Time decoding across categories is inconsistent. *A decoder was trained on start data and tested on goal data. Data at the start and at the goal were split in 30 time bins. Error bars denote standard error of the mean over trials. Each plot corresponds to one session. Different sessions show related, reversed, or no trend.*

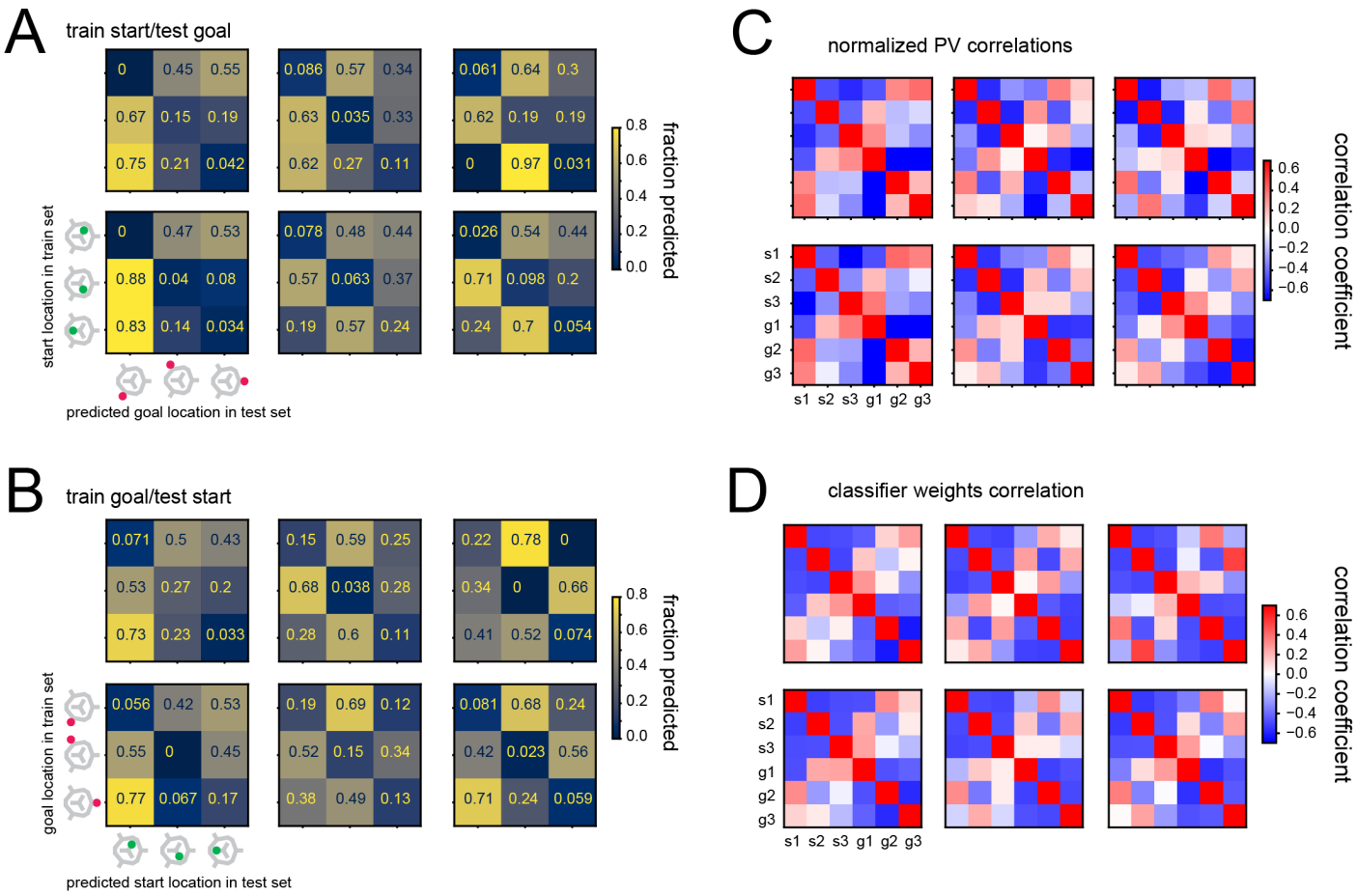

Supplementary Figure 5. Start and goal locations have structured representations reflecting the physical world, A*, predicting goal location with a classifier trained on start locations. Opposite locations (along the diagonal) were rarely predicted.* ***B****, predicting goal location with a classifier trained on start locations. Again, opposite locations were rarely predicted.* ***C****, Correlation coefficients of population vectors of start and goal locations (the goal location and start location population vectors of all trials were standardized separately before correlation to reveal any structure beyond the high similarity among start and goal location population vectors, respectively).* ***D*** *Correlation of classifier weights obtained by separately training classifiers on start or goal locations. The six correlation matrices in each panel correspond to each of the six recording sessions. In C and D, the diagonals of the lower left and upper right 3x3 blocks in each matrix have low values, revealing that the activity at starts and goals opposite each other are least similar, as seen in A and B.*

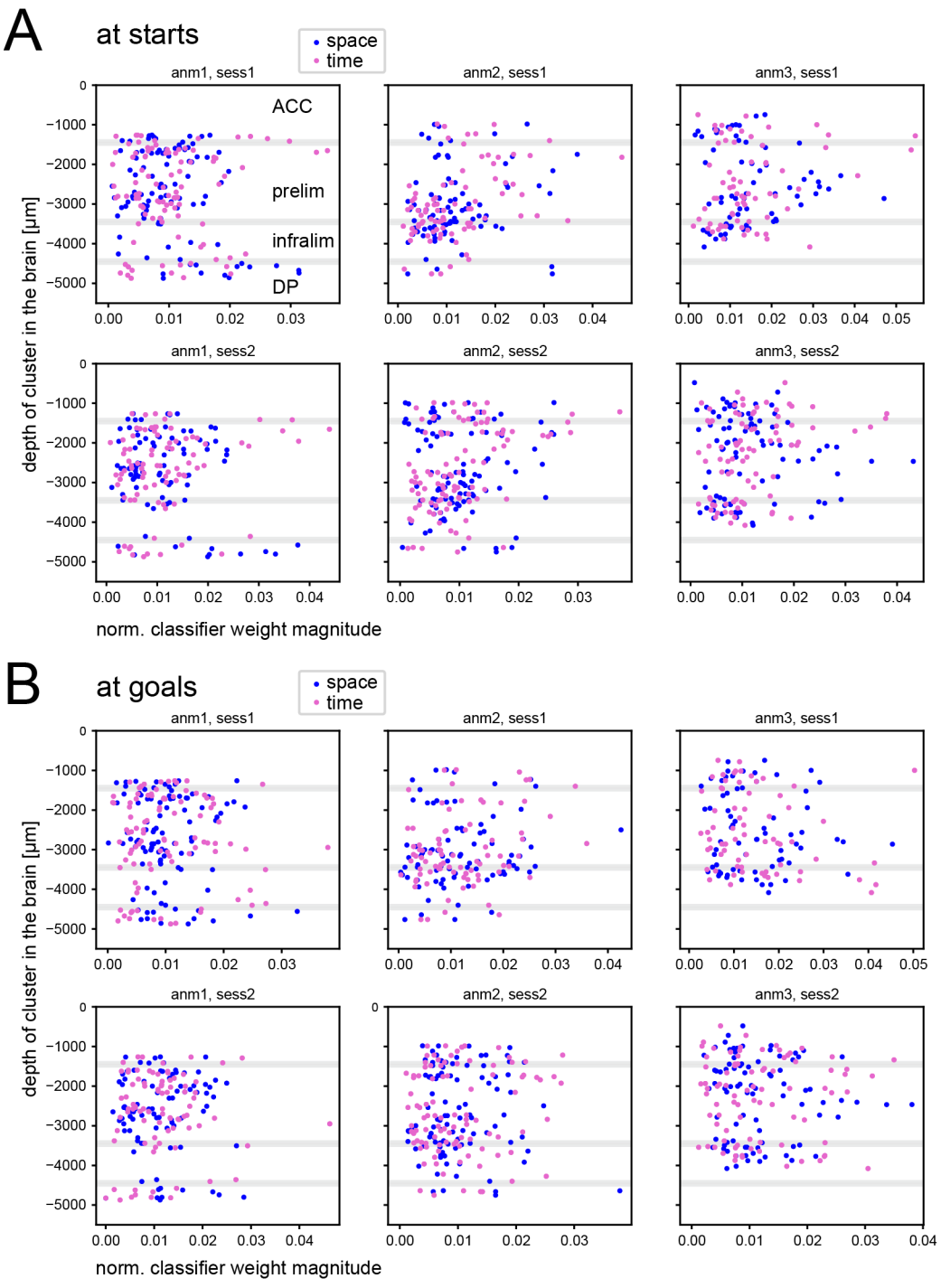

Supplementary Figure 6. Anatomical distribution of space and time selectivity. *Normalized classifier weights for all cells for space (blue) and time decoding (pink) versus depth of recording from the pial surface. Each scatter plot corresponds to one session.* ***A****, at starts,* ***B****, at goals. Divisions between subareas are estimates.*